Iranian Journal of Materials Forming 7 (1) (2020) 92-99

IJMF

Online ISSN: 2383-0042

Iranian Journal of Materials Forming

Journal Homepage: http://ijmf.shirazu.ac.ir

Microstructure and Mechanical Properties of Cold Rolled AISI 304L and 316L Austenitic Stainless Steels during Reversion Annealing

M. J. Sohrabi, H. Mirzadeh* and Ch. Dehghanian

School of Metallurgy and Materials Engineering, College of Engineering, University of Tehran, Tehran, Iran

ARTICLE INFO

Article history:

Received 11 November 2019
Revised 17 March 2020
Accepted 25 March 2020

Keywords:

Metastable austenitic steels
Martensite reversion
Microstructure
Mechanical properties
TRIP effect

ABSTRACT

Microstructural evolutions during annealing of cold rolled AISI 304L and AISI 316L stainless steels were studied. Cold rolled AISI 304L alloy was fully martensitic but cold rolled AISI 316L alloy was partially martensitic due to the higher stability of the austenite phase in the latter. During continuous heating to elevated temperatures, the complete reversion of strain-induced martensite at 750°C and an average austenite grain size of 0.4 µm was achieved in AISI 304L alloy. However, the complete reversion in AISI 316L alloy was observed at 800°C, but the recrystallization of the retained austenite was achieved at 900°C. The latter requirement for the formation of an equiaxed microstructure resulted in a much coarser average austenite grain size (2.3 µm). Annealing up to higher temperatures resulted in the grain growth of both alloys. The transformation-induced plasticity (TRIP) effect was found to be a major factor in dictating the mechanical properties, where lower stability of the austenite phase and the pronounced TRIP effect in AISI 304L alloy resulted in higher ductility in the tension test, higher friction stress in the Hall-Petch plot for hardness, and deeper dimples on the fracture surface.

1. Introduction

Techniques such as the severe plastic deformation [1-3], recrystallization [4-6], and reversion of strain-induced martensite [7-9] have been used so far for the grain refinement of austenitic stainless steels (ASSs). The last technique is based on the metastability of the austenite phase against the strain-induced martensitic transformation during deformation and the subsequent reversion of the martensite to ultrafine grained (UFG) austenite during annealing at elevated temperatures [10].

The stability of the austenite phase is important for grain refinement, where almost complete martensitic microstructure is required before reversion annealing [7, 11, 12]. Moreover, the transformation-induced plasticity (TRIP) effect, which is responsible for enhanced ductility during deformation, is dependent on the stability of the austenite phase [7]. Due to the difference in the chemical composition of AISI 304L and 316L stainless steels, the stability of the austenite phase against the martensitic transformation during deformation is different [13].

Formation of martensite, reversion, and recrystallization in AISI 304L and 316L alloys were investigated by Herrera et al. [14]. Both strain hardening and the amount of the formed martensite were higher in 304L steel and also at lower temperatures. 316L steel mounted higher resistance to recrystallization compared

* Corresponding author
E-mail address: hmirzadeh@ut.ac.ir (H. Mirzadeh).

to 304L steel. In another study by Odnobokova et al. [15], the microstructure evolution and mechanical properties of AISI 304L and 316L stainless steels subject to large strain cold bar rolling and subsequent annealing were studied, where the cold working was accompanied by mechanical twinning and strain-induced martensitic transformation. The latter was readily developed in 304L stainless steel. The subsequent annealing at temperatures above 700°C was accompanied by the martensite-austenite reversion followed by recrystallization, leading to ultrafine grained austenite. In a cold rolling study, Hadji and Badji [16] noted the contribution of both strain-induced martensite and grain size strengthening in the case of AISI 304 stainless steel, while only grain size contribution was found in the case of AISI 316 stainless steel. Shrinivas et al. [17] showed that the amount of martensite increased with an increase in the amount of rolling deformation in both AISI 304 and 316 stainless steels for a given grain size. The volume fraction of martensite increased with a decrease in grain size in AISI 304 alloy, while the martensite formation was found to be grain size insensitive in AISI 316 alloy. The volume fraction of martensite in AISI 304 alloy was always higher than that in AISI 316 alloy for a fixed percent reduction in thickness and grain size, which was attributed to the higher number of shear band intersections observed in the former alloy, which are considered to be the nucleation sites for the martensite embryos.

In addition to these works, the systematic comparison of the tensile properties of AISI 304L and 316L alloys needs more experimental works. Besides, the microstructural evolutions during annealing to control the mechanical properties of these steels need further attention in a comparative manner. Accordingly, the present work is dedicated to the study of these subjects. For this purpose, the continuous heating of cold rolled AISI 304L and 316L alloys was studied, bearing in mind that this processing route has not been applied in previous research works.

2. Experimental Details

2.1. Processing

AISI 304L and 316L stainless steel sheets with the chemical compositions shown in Table 1 were achieved in the 80% room-temperature rolled state. The average strain rate during the multi-pass rolling process was determined from Eq. (1) [18]:

$$\dot{\varepsilon} = V\sqrt{r}(1+r/4)/\sqrt{Rh_1} \quad (1)$$

where V is the peripheral speed of roll (0.086 m/s), r is the pass reduction (0.1), R is the radius of the roll (0.055 m), and h_1 is the strip thickness at entry to pass (0.055 m). Accordingly, the average rolling strain rate was determined as ~1.7 s^{-1}. The sheets were then continuously heated from room temperature up to 1150°C at the heating rate of 5°C/min, where the samples were immediately water quenched once they reached the desired temperature during heating. Fig. 1 shows a schematic representation of the applied processing route is this work.

Table 1. Chemical composition (wt.%) of alloys

Alloy	C	Cr	Ni	Mn	Mo	Fe
AISI 304L	0.01	18.6	8.3	1.4	0.1	balance
AISI 316L	0.01	17.3	10.1	1.0	2.0	balance

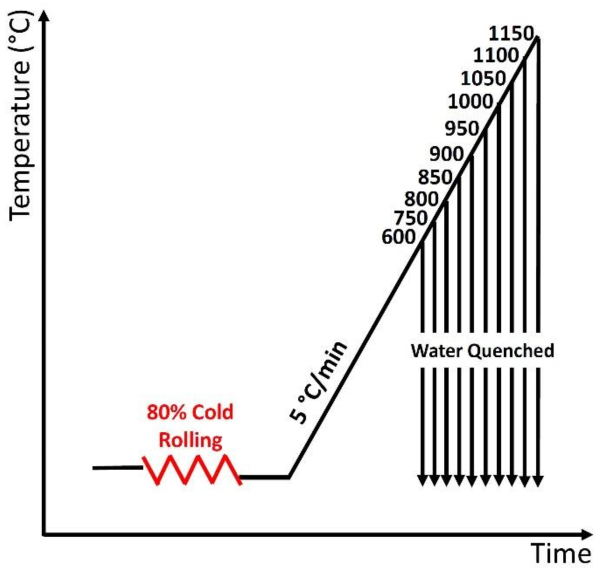

Fig. 1. schematic representation of the applied processing route is this work.

2.2. Characterization

After electrolytic polishing (H_3PO_4-H_2SO_4 solution at 40 V for 40 s) and electroetching (60% HNO_3 solution at 2 V for 20 s), the field-emission scanning electron microscopy (FEI NOVA NANOSEM 450 FE-SEM) was used for microstructural analysis. Phase identification was performed by the X-ray diffraction (XRD) technique using a PHILIPS diffractometer with Cu-kα radiation and X'Pert HighScore Plus software, where the 2θ angles between 30 and 100°, the step size of 0.02°, and the scan rate of 3°/min were employed. Based on the diffraction peaks, the amount of martensite was calculated by Eq. (2) [19]:

$$f_{\alpha'} = I_{(211)\alpha'} / \{ I_{(211)\alpha'} + 0.65 (I_{(311)\gamma} + I_{(220)\gamma}) \} \qquad (2)$$

The grain size was measured based on the standard intercept method. Hardness test was performed based on the Vickers hardness using a load of 5 kg and considering an average of five points. Tensile samples were prepared based on the subsize ASTM-E8 standard with a gauge length of 25 mm. Room temperature tensile tests were carried out using the constant cross-head speed of 1 mm/min which corresponded to the initial strain rate of ~ 0.0007 s^{-1}. As the strain rate sensitivity of the studied materials at room temperature was very low (m < 0.015) [20], the effect of the strain rate on the mechanical properties and TRIP effect was negligible and it was not considered in this work. Finally, the same FE-SEM was used for the fractographic analysis of the fractured tensile samples.

3. Results and discussion

3.1. Microstructural and phase analyses

Figure 2 shows the XRD pattern of the selected samples after continuous heating, where the amount of martensite was calculated based on Eq. (2).

The martensite content of rolled AISI 304L and 316L alloys was 95 and 52 vol%, respectively. This difference is related to the higher stability of the austenite phase in AISI 316L alloy as can be confirmed based on the M_{d30} temperature (Eq. (3)) [21]:

$$M_{d30} = 824 - 462(C+N) - 9.2Si - 8.1Mn - 13.7Cr$$
$$- 29(Ni+Cu) - 18.5Mo - 68Nb - 1.42(Gs-8) \qquad (3)$$

where M_{d30} is the deformation temperature (expressed in Kelvin) at which 50 vol% strain-induced martensite is formed by true tensile strain of 0.3, Gs is the ASTM grain size number, and all the elements are expressed in weight percent. The $Md_{30/50}$ temperature of AISI 304L and 316L alloys were calculated to be 18.8°C and -54.73 °C, respectively. This reveals the higher stability of the austenite phase against the martensitic transformation in AISI 316L alloy.

It can be seen that cold rolled AISI 304L alloy is nearly completely martensitic, but AISI 316L alloy is partially martensitic. This made it possible to study the behavior of both deformed retained austenite and martensite during annealing. For both alloys, the intensity of the diffraction peaks of martensite decreased and that of the austenite peaks increased during annealing, indicating the transformation of the strain-induced martensite to austenite (reversion). For instance, in the case of the annealed AISI 304L sample at 600°C, while the intensity of the (110) peak was higher than that of the cold rolled sample, the intensities of the rest of the martensite peaks decreased considerably and the intensities of the austenite peaks increased. The outcome was the decrease in the amount of martensite based on Eq. (2). By increasing the temperature, the fully austenitic microstructure was achieved at 750°C and 800°C for AISI 304L and 316L alloys, respectively.

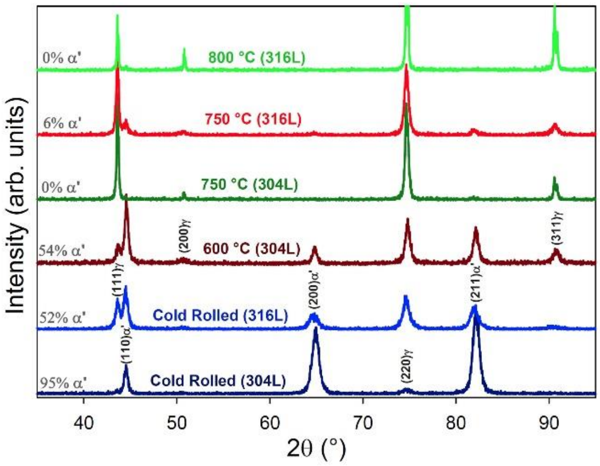

Fig. 2. XRD pattern of continuously heated samples.

The microstructure of continuously heated samples is shown in Fig. 3. Elongated grains can be seen for the rolled AISI 304L alloy in Fig. 3(a), and the XRD results of Fig. 2 reveal that these are martensite grains. Some elongated regions remained at 600°C (Fig. 3(b)), but some ultrafine grains were identified in the rest of the microstructure (Fig. 3(e)). The former is the retained martensite (54 vol%) and the latter is the reversed austenite. While the etching technique was not able to reveal the features of the martensitic regions, the XRD pattern of Fig. 2 confirms the presence of the martensite phase. At 750°C, a fully reversed microstructure with an average grain size of 0.4 μm was observed (Fig. 3(c)).

Continued heating to higher temperatures resulted in grain growth, where the average grain size of 2.74 μm was obtained at 850°C (Fig. 3(d)). For the rolled AISI 316L alloy, the pancaked grains are visible in Fig. 3(f), where these are both martensite and austenite ones. Again, the martensite and austenite phases could not be distinguished due to the nature of the employed etching technique. At 800°C, where complete reversion was achieved, some elongated retained austenite grains remained, but ultrafine grains can be seen in the rest of the microstructure (Fig. 3(g)). At 900°C, a completely recrystallized microstructure [22] with an average grain size of 2.3 μm was obtained (Fig. 3(h)). On the whole, the first equiaxed microstructure in AISI 304L and 316L alloys showed the average grain size of 0.4 and 2.3 μm, respectively. This implies the importance of the availability of a completely martensitic microstructure to obtain UFG structure upon annealing.

The average grain size and the measured hardness of fully recrystallized samples are summarized in Fig. 4. It can be seen that the hardness decreases by increasing the continuous heating temperature due to the grain coarsening.

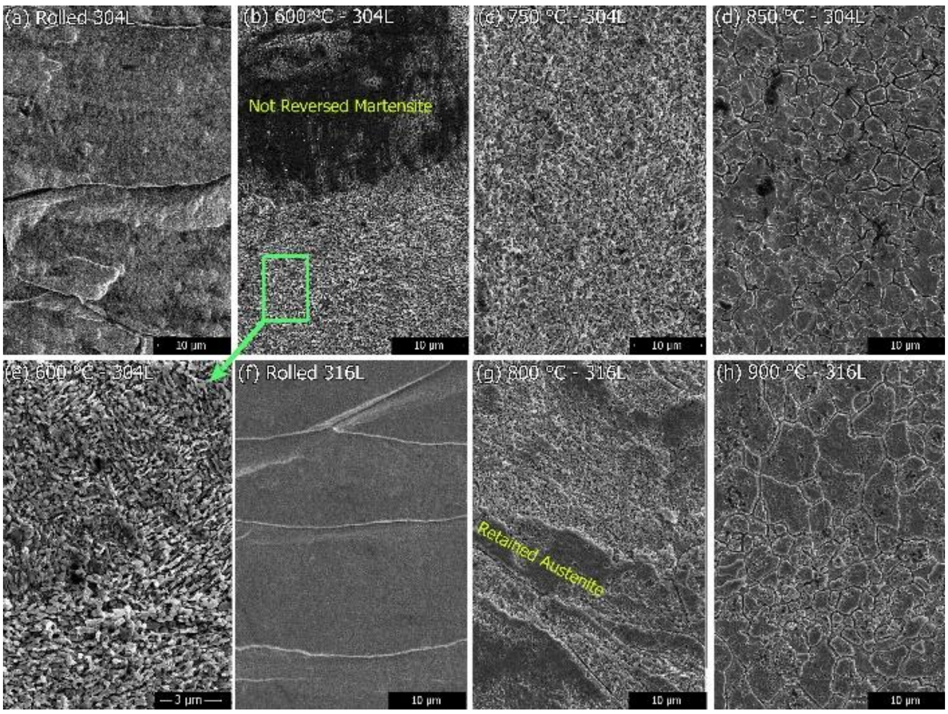

Fig. 3. Representative microstructure of continuously heated samples.

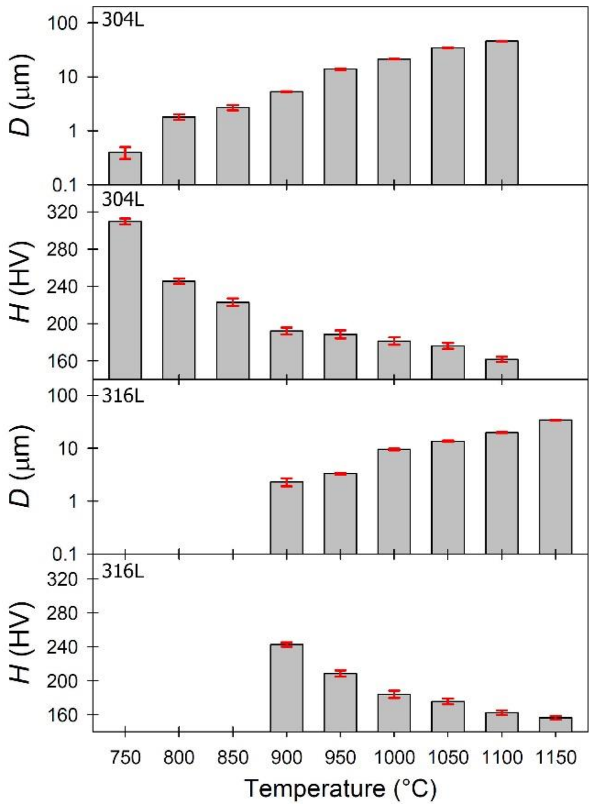

Fig. 4. Average grain size (*D*) and measured hardness (*H*) of fully recrystallized samples (quenched at various temperatures during continuous heating).

3.2. Mechanical properties

Based on Fig. 4, the Hall-Petch plots [23, 24] for the hardness of AISI 304L and 316L alloys were drawn as shown in Fig. 5. The Hall-Petch slope for both alloys is nearly the same but the intercept of the line (i.e. the friction hardness) for AISI 304L is larger despite the fact that AISI 316L alloy has higher amounts of alloying elements. It is well known that the hardness depends on both the strength and work-hardening behavior of the material [25]. Therefore, these observations might be related to the difference in the work-hardening behaviors of AISI 304L and 316L alloys, which will be discussed later.

The tensile tests were performed on AISI 304L alloy quenched at 850°C and on AISI 316L alloy quenched at 900°C, where these samples had comparable average grain sizes (Fig. 4). The results are shown in Fig. 6(a). It can be seen that these samples have nearly the same yield stress but the ultimate tensile strength (UTS) and total elongation of AISI 304L alloy are larger, which is indicative of its better work-hardening behavior. This is consistent with the hardness results in Fig. 5. Moreover, the fracture surface of AISI 304L alloy in Fig. 6(b) shows much deeper dimples compared to that of AISI 316L alloy in Fig. 6(c), which is another evidence for the enhanced plasticity of the former.

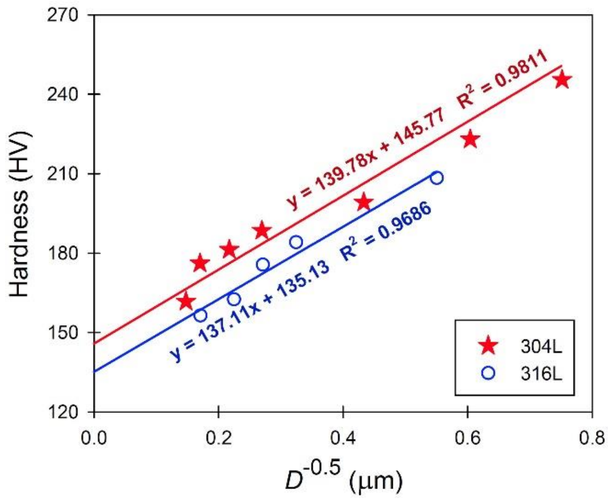

Fig. 5. Hall-Petch plots for the hardness of AISI 304L and 316L alloys.

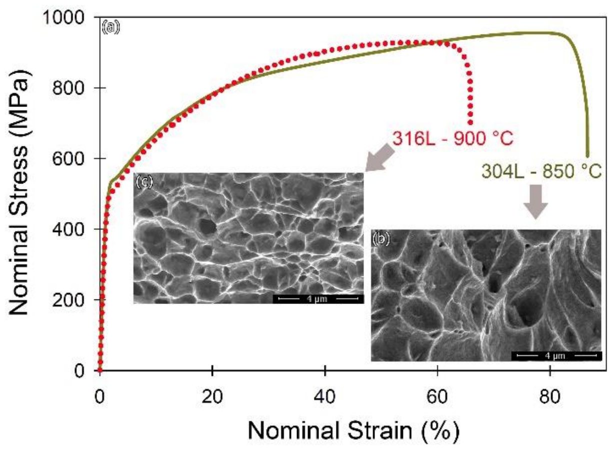

Fig. 6. Tensile stress-strain curves and the corresponding fracture surfaces.

To study the source of the increment in the work-hardening rate the XRD patterns, taken from the deformed gauge section near the necked region, were taken into account (Fig. 7). The patterns show that the amount of the formed strain-induced martensite during the tension test was much higher in AISI 304L alloy, implying that the transformation-induced plasticity (TRIP) effect was prevalent in this sample. However, during the tension of AISI 316L alloy, the amount of the formed martensite was low, which is related to the higher stability of the austenite phase in this alloy as discussed before.

The occurrence of the TRIP effect is responsible for the delayed necking in the tension test, which enhances the ductility of the alloy. This manifested itself in the form of higher ductility in the tension test, higher friction stress in the Hall-Petch plot for hardness, and deeper dimples on the fracture surface of AISI 304L alloy.

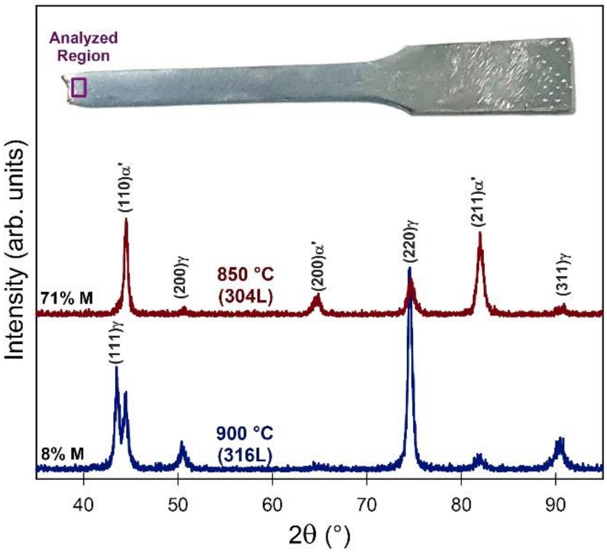

Fig. 7. XRD patterns taken from the deformed gauge section near the necked region.

4. Conclusions

Microstructural evolutions during the annealing of cold rolled AISI 304L and 316L stainless steels were studied. The following conclusions can be drawn:

1- Cold rolled AISI 304L alloy was fully martensitic but cold rolled AISI 316L alloy was partially martensitic due to the higher stability of the austenite phase in the latter.

2- During continuous heating to elevated temperatures, the complete reversion of strain-induced martensite at 750 °C and an average austenite grain size of 0.4 µm was achieved in AISI 304L alloy. However, the complete reversion in AISI 316L alloy was observed at 800°C, but the recrystallization of the retained austenite was achieved at 900°C. The latter requirement for the formation of an equiaxed microstructure resulted in a much coarser average austenite grain size (2.3 µm). Annealing up to higher temperatures resulted in the grain growth of both alloys.

3- The transformation-induced plasticity (TRIP) effect was found to be a major factor in dictating the mechanical properties, where lower stability of the austenite phase and the pronounced TRIP effect in AISI 304L alloy resulted in higher ductility in the tension test, higher friction stress in the Hall-Petch plot for hardness, and deeper dimples on the fracture surface.

5. References

[1] S. Sabooni, F. Karimzadeh, M.H. Enayati, A.H.W. Ngan, Friction-stir welding of ultrafine grained austenitic 304L stainless steel produced by martensitic thermomechanical processing, *Materials and Design* 76 (2015) 130-140.

[2] X. H. Chen, J. Lu, L. Lu, and K. Lu, Tensile properties of a nanocrystalline 316L austenitic stainless steel, *Scripta Materialia 52* (2005) 1039-1044.

[3] M. V. Karavaeva, M. M. Abramova, N. A. Enikeev, G. I. Raab, R. Z. Valiev, Superior strength of austenitic steel produced by combined processing, including equal-channel angular pressing and rolling, *Metals* 6 (2016) 310.

[4] H. Mirzadeh, J. M. Cabrera, A. Najafizadeh, P. R. Calvillo, EBSD Study of a Hot Deformed Austenitic Stainless Steel, *Materials Science and Engineering: A* 538 (2012) 236-245.

[5] S. Mandal, A. K. Bhaduri, V. S. Sarma, A study on microstructural evolution and dynamic recrystallization during isothermal deformation of a Ti-modified austenitic stainless steel, *Metallurgical and Materials Transactions A* 42 (2011) 1062-1072.

[6] M. B. R. Silva, J. Gallego, J. M. Cabrera, O. Balancin, A. M. Jorge Jr, Interaction between recrystallization and strain-induced precipitation in a high Nb-and N-bearing austenitic stainless steel: Influence of the interpass time, *Materials Science and Engineering: A* 637 (2015) 189-200.

[7] S. Kheiri, H. Mirzadeh, M. Naghizadeh, Tailoring the microstructure and mechanical properties of AISI 316L austenitic stainless steel via cold rolling and reversion annealing, *Materials Science and Engineering: A* 759 (2019) 90-96.

[8] A. Amininejad, R. Jamaati, S. J. Hosseinipour, Achieving superior strength and high ductility in AISI 304 austenitic stainless steel via asymmetric cold rolling, *Materials Science and Engineering: A* 767 (2019) 138433.

[9] G. Sun, L. Du, J. Hu, B. Zhang, R. D. K. Misra, On the influence of deformation mechanism during cold and warm rolling on annealing behavior of a 304 stainless steel, *Materials Science and Engineering: A* 746 (2019) 341-355.

[10] M. J. Sohrabi, H. Mirzadeh, C. Dehghanian, Thermodynamics basis of saturation of martensite content during reversion annealing of cold rolled metastable austenitic steel, *Vacuum* 174 (2020) 109220.

[11] A. Järvenpää, M. Jaskari, A. Kisko, P. Karjalainen, Processing and Properties of Reversion-Treated Austenitic Stainless Steels, *Metals* 10 (2020) 281.

[12] S. Sadeghpour, A. Kermanpur, A. Najafizadeh, Influence of Ti microalloying on the formation of nanocrystalline structure in the 201L austenitic stainless steel during martensite thermomechanical treatment, *Materials Science and Engineering: A* 584 (2013) 177-183.

[13] M. Naghizadeh, H. Mirzadeh, Microstructural Evolutions During Reversion Annealing of Cold-Rolled AISI 316 Austenitic Stainless Steel, *Metallurgical and Materials Transactions A* 49 (2018) 2248-2256.

[14] C. Herrera, R. L. Plaut , A. F. Padilha, Microstructural Refinement during Annealing of Plastically Deformed Austenitic Stainless Steels, *Materials Science Forum* 550 (2007) 423-428.

[15] M. Odnobokova, A. Belyakov, A. Kipelova, R. Kaibyshev, Formation of ultrafine-grained structures in 304L and 316L stainless steels by recrystallization and reverse phase transformation, *Materials Science Forum* 838-839 (2016) 410-415.

[16] M. Hadji, R. Badji, Microstructure and mechanical properties of austenitic stainless steels after cold rolling, *Journal of Materials Engineering and Performance* 11 (2002) 145-151.

[17] V. Shrinivas, S. K. Varma, L. E. Murr, Deformation-induced martensitic characteristics in 304 and 316 stainless steels during room-temperature rolling, *Metallurgical and Materials Transactions A* 26 (1995) 661-671.

[18] A. A. Popoff, Simplified hot rolling load calculations incorporating material strain rates, *International Journal of Mechanical Sciences* 18 (1976) 529-532.

[19] A. Etienne, B. Radiguet, C. Genevois, J.M. Le Breton, R. Valiev, P. Pareige, Thermal stability of ultrafine-grained austenitic stainless steels, *Materials Science and Engineering: A* 527 (2010) 5805-5810.

[20] G. L. Huang, D. K. Matlock, G. Krauss, Martensite formation, strain rate sensitivity, and deformation behavior of type 304 stainless steel sheet, *Metallurgical Transactions A* 20 (1989) 1239-1246.

[21] K. Nohara, Y. Ono, N. Ohashi, Composition and grain size dependencies of strain-induced martensitic transformation in metastable austenitic stainless steels, *Tetsu-to-Hagané* 63 (1977) 772-782.

[22] Y. C. Lin, M. S. Chen, Study of microstructural evolution during static recrystallization in a low alloy steel, *Journal of Materials Science* 44 (2009) 835-842.

[23] W. Qin, J. Li, Y. Liu, J. Kang, L. Zhu, D. Shu, P. Peng, D. She, D. Meng, Y. Li, Effects of grain size on tensile property and fracture morphology of 316L stainless steel, *Materials Letters* 254 (2019) 116-119.

[24] Y. Mazaheri, F. Karimzadeh, M.H. Enayati, A novel technique for development of A356/Al_2O_3 surface nanocomposite by friction stir processing, *Journal of Materials Processing Technology* 211 (2011) 1614-1619.

[25] M.A. Meyers, K.K. Chawla, Mechanical Behavior of Materials, Second Edition, Cambridge University Press, 2009.

ریزساختار و خواص مکانیکی فولادهای زنگ نزن آستنیتی ۳۰۴ ال و ۳۱۶ ال نورد سرد شده در حین آنیل بازگشتی

محمد جواد سهرابی، حامد میرزاده، چنگیز دهقانیان

دانشکده مهندسی متالورژی و مواد، دانشکده فنی، دانشگاه تهران، تهران، ایران.

چکیـــده

تحولات ریزساختاری در حین آنیل فولادهای زنگ نزن آستنیتی ۳۰۴ ال و ۳۱۶ ال نورد سرد شده مورد مطالعه قرار گرفت. فولاد ۳۰۴ ال نورد سرد شده کاملا مارتنزیتی بود ولی فولاد ۳۱۶ ال نورد سرد شده نیمه مارتنزیتی-نیمه آستنیتی بود که به پایدارتر بودن فاز آستنیت در دومی ربط داده شد. در حین آنیل پیوسته تا دماهای بالا، بازگشت کامل مارتنزیت ناشی از کرنش در دمای ۷۵۰ درجه سلسیوس و اندازه دانه متوسط ۰/۴ میکرومتر برای فولاد ۳۰۴ ال به دست آمد. بازگشت کامل مارتنزیت در فولاد ۳۱۶ ال در دمای ۸۰۰ درجه سلسیوس رخ داد و تبلور مجدد آستنیت باقی مانده در دمای ۹۰۰ درجه سلسیوس به وقوع پیوست. این پیش نیاز برای ایجاد ساختار هم محور سبب شد که اندازه دانه متوسط بسیار بزرگتر (۲/۳ میکرومتر) برای فولاد ۳۱۶ ال به دست آید. آنیل تا دماهای بالاتر منجر به رشد دانه در هر دو آلیاژ شد. پدیده پلاستیسیته القا شده توسط استحاله به عنوان یک عامل مهم در تعیین خواص مکانیکی مطرح شد، در جایی که پایداری کمتر فاز آستنیت و پدیده پلاستیسیته القا شده توسط استحاله قوی تر در فولاد ۳۰۴ ال منجر به انعطاف پذیری بالا در حین آزمون کشش، تنش اصطکاکی شبکه بالاتر در رابطه هال-پچ، و دیمپل های عمیق تر در سطح شکست شد.

واژه‌های کلیدی: فولادهای زنگ نزن شبه پایدار، بازگشت مارتنزیت، ریزساختار، خواص مکانیکی، پدیده پلاستیسیته القا شده توسط استحاله